

Hyperspectral Remote Sensing of Canopy Biodiversity in Hawaiian Lowland Rainforests

Kimberly M. Carlson,¹ Gregory P. Asner,^{1,*} R. Flint Hughes,²
Rebecca Ostertag,³ and Roberta E. Martin¹

¹Department of Global Ecology, Carnegie Institution of Washington, 260 Panama Street, Stanford, California 94305, USA; ²Institute for Pacific Islands Forestry, USDA Forest Service, Hawaii, Hilo 96720, USA; ³Department of Biology, University of Hawai'i, Hawaii, Hilo 96720, USA

ABSTRACT

Mapping biological diversity is a high priority for conservation research, management and policy development, but few studies have provided diversity data at high spatial resolution from remote sensing. We used airborne imaging spectroscopy to map woody vascular plant species richness in lowland tropical forest ecosystems in Hawai'i. Hyperspectral signatures spanning the 400–2,500 nm wavelength range acquired by the NASA Airborne Visible and Infrared Imaging Spectrometer (AVIRIS) were analyzed at 17 forest sites with species richness values ranging from 1 to 17 species per 0.1–0.3 ha. Spatial variation (range) in the shape of the AVIRIS spectra (derivative reflectance) in wavelength regions associated with upper-canopy pigments, water, and nitrogen content were well correlated with species richness across field sites. An analysis of

leaf chlorophyll, water, and nitrogen content within and across species suggested that increasing spectral diversity was linked to increasing species richness by way of increasing biochemical diversity. A linear regression analysis showed that species richness was predicted by a combination of four biochemically-distinct wavelength observations centered at 530, 720, 1,201, and 1,523 nm ($r^2 = 0.85$, $p < 0.01$). This relationship was used to map species richness at approximately 0.1 ha resolution in lowland forest reserves throughout the study region. Future remote sensing studies of biodiversity will benefit from explicitly connecting chemical and physical properties of the organisms to remotely sensed data.

Key words: AVIRIS; biological diversity; Hawai'i; imaging spectroscopy; leaf pigments.

INTRODUCTION

Mapping biological diversity is a major goal in the global conservation community (for example, Heywood and Watson 1995; Gaston 2000). This task is daunting because ecological processes and

human activities driving genetic, species, and community distributions lead to exceedingly complex spatial patterns of biodiversity. From a conservation standpoint, fine-scale biodiversity maps (< 0.5 km resolution) are useful because these data give land managers and scientists an understanding of species distributions on a scale commensurate with conservation, management, and policy development activities. Furthermore, such maps set a starting point from which changes in the landscape can be tracked over time, giving communities feedback regarding how their management deci-

Electronic supplementary material: The online version of this article (doi:10.1007/s10021-007-9041-z) contains supplementary material, which is available to authorized users.

Received 23 May 2006; accepted 11 December 2006; published online 18 July 2007.

*Corresponding author; e-mail: gpa@stanford.edu

sions are affecting local ecosystems (Innes and Koch 1998). Fine-scale biodiversity estimates have traditionally relied on extrapolation from labor-intensive field studies (Pielou 1966; Gotelli and Colwell 2001), yet recent advances in remote sensing technology may facilitate regional-scale biodiversity mapping (Turner and others 2003).

Remote sensing of biodiversity is not new; in the past few decades researchers have applied remotely sensed data to assess biodiversity over an array of ecosystems and types of diversity, from avian species richness to vascular plant diversity (Johnson and others 1998; Nagendra 2001). The majority of these attempts use medium to coarse spatial resolution (≥ 30 m pixels), multispectral (< 10 bands) data. Regional maps produced via this combination of low spatial and spectral resolution data generally use correlations between remotely sensed land cover and biological diversity. However, for fine-scale diversity assessments, particularly in places where land cover (for example, forests) is constant and the object of study varies at fine spatial scales (for example, individual trees with small canopies), the 30-m resolution provided by Landsat and similar imagery does not adequately capture landscape and species diversity (Cohen and others 1990). The biophysical information collected by multispectral sensors is also limited because the low spectral resolution of these sensors cannot resolve details of vegetation canopy structure and chemistry. Therefore, the ability to detect canopy-level diversity in complex, layered forested areas is often limited.

Imaging spectroscopy, also called hyperspectral remote sensing, has the potential to resolve the spatial and spectral discrimination problems presented above, and to provide a biophysically-based approach for mapping biodiversity. Hyperspectral data provide detailed information on a wide range of canopy properties including canopy water content and leaf pigment, nitrogen, cellulose, and lignin concentrations (Curran 1989; Jacquemoud and others 1996). Collected at appropriate spatial resolution, hyperspectral data provide information on how chemical and structural properties of vascular plants vary within and across ecosystems (Martin and Aber 1997; Ustin and others 2004). In combination with plant chemical and structural properties, these data can be used to classify individual tree species (Clark and others 2005; Cochrane 2000).

The Hawaiian Islands are an ideal place to test the utility of such fine-scale mapping for conservation because of their importance as a "biodiversity hotspot" (Myers and others 2000), and due to the matrix of substrate ages, climate zones, and

ecosystem types found throughout the archipelago (Vitousek 2004; Asner and others 2005). In particular, lowland tropical forests on the island of Hawai'i provide a good test of whether remote sensing can be used to track the diversity of vascular plants in multi-layered forest canopies. Hawaiian forests have relatively low plant species diversity and simple forest structure compared to other tropical forests (Mueller-Dombois and Fosberg 1998), a combination that facilitates a test of remote sensing for plant species diversity mapping in a setting with good experimental control and manageable canopy complexity.

We used airborne imaging spectroscopy, field biodiversity studies, and leaf biochemical data collected in lowland forests on the island of Hawai'i to: (1) determine if high spatial resolution hyperspectral data are correlated with field-measured woody vascular plant species diversity; (2) test if airborne remote sensing signatures are linked to plant species diversity by way of leaf chemistry; (3) develop an algorithm for woody vascular plant species richness prediction in Hawaiian lowland forest ecosystems; and (4) apply this biodiversity prediction algorithm to our airborne remote sensing data to produce high-resolution, regional maps of plant species richness based on inter-pixel variation.

MATERIALS AND METHODS

Remote Sensing

On February 11 and 21, 2005, the Airborne Visible and Infrared Imaging Spectrometer (AVIRIS) collected hyperspectral imagery over our study sites on the eastern side of the island of Hawai'i in the Puna and South Hilo districts, hereafter referred to as the Puna region (Figure 1). The area is dominated by tropical moist-to-wet lowland forest with mean annual rainfall ranging from 2,000 to 4,000 mm y^{-1} and mean annual temperatures of 18–24°C (Giambelluca and others 1986; Asner and others 2005). The Puna region is a patchwork of many land uses including agricultural, residential, and protected forestlands undergoing various degrees of invasion by non-native species. All study sites are located on protected lands managed by one of three entities: the Hawai'i State Division of Forestry and Wildlife, Kamehameha Schools, and the Army National Guard.

AVIRIS measures upwelling radiance from 366 to 2,510 nm in 224 channels with a nominal 10 nm full-width at half maximum (Green and others 1998). The instrument was mounted on DASH-6

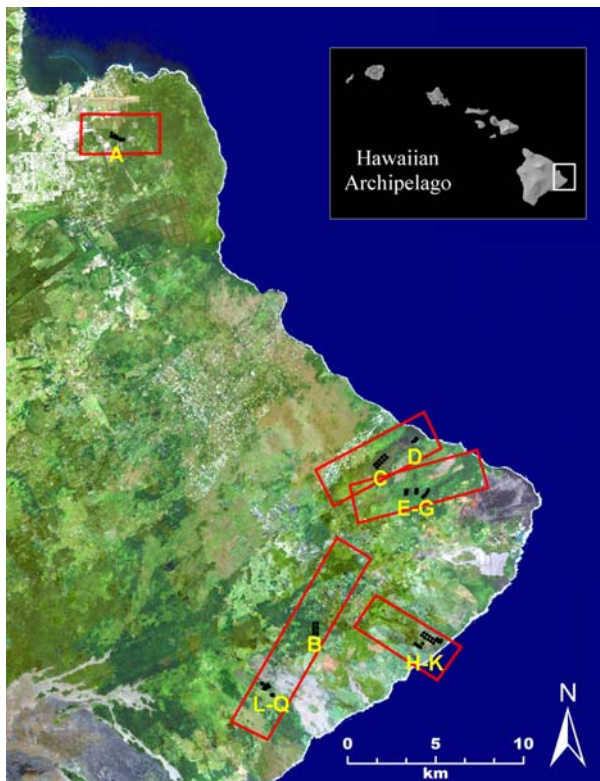


Figure 1. The southeastern portion of the Island of Hawai'i, showing location of airborne imaging spectrometer overflights (red boxes), and plots (black dots) at each field site (yellow letters).

turboprop that flew 3–4 km a.g.l. during data acquisition, resulting in a ground instantaneous field-of-view (GIFOV) of 3.3–3.6 m. All images were acquired between 1,200 and 1,400 h local time. Five images totaling 95 km² were sufficient to cover our study sites (Figure 1).

We used the ACORN-5 Mode 1.5 atmospheric correction code, which estimates water vapor on a pixel-by-pixel basis, to correct radiance data to apparent surface reflectance (ImSpec Inc., Palm-dale, California, USA). Wavelengths used for water vapor retrieval were centered at the 940 and 1,140 nm features. The ACORN code estimated visibility throughout the image, and a humid tropical atmosphere was used for the simulation. No ground target was used to improve reflectance retrieval. AVIRIS high-resolution data are subject to a number of artifacts that can produce high frequency noise and increase reflectance data range. Because our analysis depends heavily on variation in reflectance range, we chose to employ artifact suppression in ACORN-5, and also to mask wavelengths from 1,344 to 1,408 and 1,793–2,008 nm, which are dominated by atmospheric

water absorption. This resulted in 194 channels of useable data spanning the 366–2,510 nm wavelength range. In addition to the calibrated reflectance imagery, we also worked with the derivative of the spectral signatures, which normalizes for brightness effects and gives further information about the shape of the spectral curve. These derivative reflectance spectra, calculated using a finite differencing algorithm, were not smoothed.

Preliminary geo-registration of all data was performed using the inertial navigation system data taken onboard the aircraft. The images were further geo-rectified using Landsat GeoCover data (<http://www.glc.umd.edu/portal/geocover/>) and geographic information system (GIS) layers provided by the State of Hawai'i (<http://www.hawaii.gov/dbedt/gis/>). We then mosaicked the five-reflectance and derivative-reflectance images and re-sampled all images using a nearest-neighbor method to 3.6 m, which was the largest pixel size among the five AVIRIS flightlines. Past spatial scaling analyses exploring optimal pixel size for hyperspectral ecosystem studies suggest that optimal spatial scale can vary widely and is highly dependent on the ecological feature being studied (Rahman and others 2003). Generally, effective sampling requires that the sample is at least one-half the width of the object (McGrew and Monroe 2000). In the Puna region, the 3.6 m pixel size is appropriate to sense variation in species-level diversity because individual plant canopies in the Puna region average 8–20 m in diameter (Asner and Hughes, unpublished data).

Field Diversity Data

The study sites were chosen throughout lowland forests in the Puna region to span a range of species richness levels (Figure 1). Because the number of tropical woody species increases with time since catastrophic disturbance (for example, lava flows) and with soil fertility (Givnish 1999), we chose sites on a single substrate type—Kilauea volcano tholeiitic basalt lava flows—but across a range of substrate ages from 51 to 750–1,500 years old (Moore and Trusdell 1991; Table 1). Thus our study design relies on the fact that, in the Puna region of Hawaii, species richness tends to increase as substrate age increases.

We collected woody species richness and stem density data at 17 sites in 2001, 2003–2004, and 2006. At each site, between 9 and 11 plot centers were placed at regular intervals on a single lava flow age and under consistent canopy cover. Plots were sampled using a nested design. The 2001 data

Table 1. List of Study Sites, Labeled A–Q

Site Code	Site Name	Substrate Age (ybp)	Plots (#)	Site Area (m ²)	Species Richness (# species)	Shannon Diversity (H')	Non-native Area (%)	Non-native Basal Stems (%)
A	Keaukaha Military Reservation	750–1,500	10	2,545	17	1.57	34	87
B	Puu Kaliu Brysons Forest Reserve	450–750	8	2,036	17	1.94	7	62
C	Nanawale Military Reservation	166	11	2,799	6	0.14	0	1
D	Nanawale Forest Reserve	166	10	2,545	14	1.56	90	90
E	Nanawale Forest Reserve	200–400	10	2,545	17	2.01	38	86
F	Nanawale Forest Reserve	400–750	10	2,545	15	2.00	11	54
G	Nanawale Forest Reserve	750–1,500	10	2,545	10	1.11	14	86
H	Malama Ki Forest Reserve	216	10	2,545	9	0.56	9	9
I	Malama Ki Forest Reserve	400–750	9	2,290	13	1.71	16	73
J	Malama Ki Forest Reserve	216	10	999	6	0.40	1	2
K	Malama Ki Forest Reserve	216	10	999	10	1.32	94	90
L	Keauohana Forest Reserve	51	10	999	1	0.00	0	0
M	Keauohana Forest Reserve	51	10	999	7	1.09	99	78
N	Keauohana Forest Reserve	200–400	10	999	6	0.77	23	85
O	Keauohana Forest Reserve	200–400	11	1,099	7	1.22	61	74
P	Keauohana Forest Reserve	200–400	10	999	9	1.04	0	6
Q	Keauohana Forest Reserve	200–400	10	999	7	1.08	10	68
Totals			169	30,488	44	2.21	30	69

were collected for a previous study, and sample design and methods for these data differ slightly from the data collected from 2003–2006. In 2001, 5.64-m radius plots were sampled using the method outlined in Hughes and Denslow (2005). In 2003–2004 and 2006, plots were sampled using the following method: in an 18-m radius circle, all woody stems with a diameter at breast height (DBH) greater than or equal to 30 cm were counted and species recorded. In a 9-m radius circle, all stems with a DBH greater than or equal to 2 cm were counted and species recorded. In a 6-m radius circle, all stems with a DBH less than 2 cm but greater than or equal to 1.3 m in height were counted and species recorded. We then calculated woody species richness and the Shannon Diversity index ($H' = -\sum p_i \ln(p_i)$, where p_i is the proportional abundance of the i th species), based on stem abundance field data at each site (Pielou 1966).

In addition to species data, we collected high-precision geo-location data at each plot center using a Leica 50+ global positioning system (GPS) unit (Leica Geosystems Inc., St Gallen, Switzerland). The GPS data were differentially corrected using local base station data for more accurate point location. A few plot center coordinates could not be collected using the GPS unit. In these cases, plot coordinates were calculated based on a distance and bearing from a known GPS coordinate.

Leaf Biochemical Data

Although past studies have connected spectral variation from remote sensing to field-measured plant species diversity, the biophysical basis for such relationships has not been firmly established. To examine how leaf biochemical variation may be linked to hyperspectral observations, we gathered leaf-level data for a subset of the study sites and species selected from the field biodiversity surveys. Using these leaf collections, we then quantified and compared intra- and inter-species variation in leaf chlorophyll, water, and nitrogen content, leaf-level properties that have been shown to influence AVIRIS spectra (Ustin and others 2004).

In May and June 2005, we collected top-of-canopy leaves from 200 individual plants at sites across the Puna region using a shotgun. Small branches of each species were collected from fully sunlit portions of the canopies and stored in plastic bags on ice for transport to a nearby laboratory. Samples (35–75 leaves) were scanned for leaf area determination and weighed within 2 h of collection. Foliar samples were dried at 70°C for at least 72 h and weighed to determine percent water

content and specific leaf area (SLA; $\text{cm}^2 \text{g}^{-1}$). Dried leaves were then ground in a 20-mesh Wiley mill, and subsets analyzed for nitrogen (N) content using a standard Kjeldahl sulfuric acid/cupric sulfate digest. Digests were analyzed using an Alpkem autoanalyzer (O-I Analytical, College Station, Texas, USA).

Three leaves from each original, fresh sample were immediately frozen and stored at -80°C for pigment analyses. Frozen leaf discs (3 each, 1.13 cm^2 total area) were ground in 100% acetone in a chilled mortar, with a small amount of quartz sand and MgCO_3 added to prevent acidification. Following centrifugation for 3 min at 3,000 rpm, the absorbance of the supernatant was measured using a dual beam scanning UV–VIS spectrophotometer (Lambda 25, Perkin Elmer Ltd., Beaconsfield, UK). Chlorophyll *a* and *b* content were determined according to Lichtenthaler (1987) and Lichtenthaler and Buschmann (2001), using a multi-wavelength analysis at 470, 645, 662 and 710 nm. For this study, chlorophyll *a* and *b* were summed for a single measurement of total chlorophyll concentration.

Foliar measurements of water, total chlorophyll and nitrogen were expressed on an area basis by dividing measured biochemical concentration by SLA. This resulted in leaf biochemical units of equivalent water thickness (EWT mm), leaf chlorophyll content (total chlorophyll, $\mu\text{g cm}^{-2}$) and leaf nitrogen content ($\text{N } \mu\text{g cm}^{-2}$). We then computed the mean value of each biochemical property for all samples collected by species and/or by site (Appendix 1, see <http://www.springerlink.com>).

Monte-Carlo Simulation

We used a Monte-Carlo simulation technique to understand how variation in leaf-level constituents changes with species richness. The technique involved a simple calculation of the changing range of biochemical values as each new species is added to a sample population. First, a single species was randomly selected from the total population of n species, and the mean biochemical property was recorded (for example, total chlorophyll). Thereafter, other species were randomly selected and combined with the previously selected species to track the change in the total range (maximum–minimum) of biochemical values as the sample size increased. These random selections of species were repeated until the entire population was sampled. This procedure was carried out 1,000 times, and the average change in the value range of the increasing sample population was calculated. This model was

run for each individual metric of EWT, total chlorophyll, and N, as well as for an index (Λ) that combined all three leaf chemical properties per species (i). This index was calculated as the square root of the sum of squared normalized values of all three parameters:

$$\Lambda_i = \sqrt{[(EWT_i/EWT_{\max})^2 + (Chl_i/Chl_{\max})^2 + (N_i/N_{\max})^2]} \quad (1)$$

We used these data to show how ranges of leaf water, chlorophyll and nitrogen content change with species richness ($i = 1$ to n). We also repeated the effort for the mean values of *Metrosideros polymorpha*, a native tree that is dominant across rainfall, elevation, and substrate gradients in Hawai'i (Vitousek 2004), and which was found at all nine of the leaf collection sites (Appendix 2, see <http://www.springerlink.com>). This allowed us to quantify the intra-species variation of leaf biochemical properties for *M. polymorpha* in comparison to variation across species.

Biodiversity Prediction

We chose to analyze both spectral and field data on a site-by-site basis because the geo-location error (± 2 pixels) was larger than the smallest plots. The mean reflectance M_{Refl} , range of reflectance R_{Refl} , mean first derivative of reflectance M_{Deriv} , and range of the first derivative of reflectance R_{Deriv} were calculated at each sample site. These values were derived from circular areas centered on each field plot and had the same radius as the survey plot (either a 9 m or 5.64 m). By sampling spectral data from plots with the same area as field data plots, differences in plot size were effectively normalized.

We were able to use the range of spectral values at each wavelength, instead of other available metrics, such as standard deviation or skewness, because AVIRIS data have a very high signal-to-noise ratio. Range captures spectral outliers better than mean-based measures such as standard deviation, thus we found this spectral measurement to be highly sensitive to occasional species, just as field-measured species richness is sensitive to rare species.

To determine whether linear relationships exist between field diversity and spectral data, we computed Pearson's correlation coefficients (r) between the two diversity measurements (species richness and H') and the four spectral measurements (M_{Refl} , R_{Refl} , M_{Deriv} , and R_{Deriv}) at each wavelength. Using

significantly related reflectance and derivative mean and range wavelengths as determined by correlation analysis, as well as biophysical knowledge of information contained in different regions of the spectrum, we then developed a simple biodiversity prediction algorithm using linear regression analysis. This involved the use of a combination of narrow spectral bands available from AVIRIS.

Finally, we applied this algorithm to the AVIRIS imagery, creating a map of estimated woody species richness per area across five protected areas in the Puna region of Hawai'i. To do so, we calculated the range of the derivative spectra in a moving 9×9 pixel (~ 0.1 ha) cluster or kernel across the image, so that each pixel was assigned a range spectrum based on the minimum and maximum values at each wavelength within each cluster of pixels. We then calculated the woody species richness of each pixel using the diversity prediction algorithm developed above. These values represent total richness in the approximately 0.1 ha area surrounding each pixel. Because anthropogenic edges may introduce spectral variation not linked to species richness, we masked a 26 m distance to each side of all man-made features (in this case, roads) intersecting with reserves, as well as reserve edges. Thus any pixel whose richness estimate included a road or reserve edge was excluded from calculations. We then extracted mean species richness per unit area in these masked reserve areas of the Puna region.

RESULTS AND DISCUSSION

Field Diversity Measurements

Forty-four woody vascular plant species were recorded across the 17 sites (Appendix 2, see <http://www.springerlink.com>). Of these, the majority of species (23) were classified as natives, 20 were non-native species, and one was unknown. Across all sites, non-native species accounted for 30% of total basal area and 69% of total stems (Table 1). Dominant species in terms of basal area were native *M. polymorpha* (53%) and non-native *Casuarina equisetifolia* (10%). The largest percentage of stems was measured among non-natives *Psidium cattleianum* (30%) and *Melastoma candidum* (12%), and native *M. polymorpha* (27%). Discrepancies between basal area and stem abundance dominance are important: at sites where dominant species composition in terms of basal area differs from dominant species composition in terms of stem abundance, canopy species composition may

also differ from understory species composition. For example when native basal area is high and native stem abundance is low, a site may have mostly native overstory and mostly nonnative understory. Therefore, any attempt at mapping total species richness in this region must consider both overstory and understory species richness.

Stem counts at each site highlighted a clear division between highly non-native (>50% stems non-native, 12 sites) or native (<10% of stems non-native, 5 sites) communities. This division between “native” and “non-native” stands is notable because it demonstrates that some forests in the Puna region are still mostly native, which highlights the importance of establishing a baseline biodiversity map here. Such a map would allow local land managers to track the effects of non-native species on biodiversity in the area.

The number of woody vascular plant species recorded at each site ranged from 1 to 17, and H' values ranged from 0 to 2.01 (Table 1). Although we tried to sample in a way that would capture the total woody species richness in the broader vegetation/substrate age area surrounding each sample site, species-area curves constructed at each site showed that we did not sample to species saturation in most cases (except for sites F, L, and Q; Figure 2). The approximately 0.1 ha plots show particularly steep species-area curves, thus we cannot extrapolate plot-level species richness values to the broader stand or ecosystem levels. However, it was still valid to sample the remote sensing data within these plots to link to biodiversity at that scale.

Correlation Analysis

Large variations in the mean (M_{Refl}) and derivative (M_{Deriv}) spectra were observed in the AVIRIS data collected across study sites (Figure 3). However, Pearson correlation analysis between species richness and spectral data indicated that M_{Refl} and M_{Deriv} were weakly correlated with species richness across most of the spectrum (Figure 4A–B). Therefore, the brightness and shape of the spectrum at any given wavelength is generally a poor predictor of woody plant richness in these lowland tropical forest systems.

In contrast, the reflectance and derivative-reflectance ranges (R_{Refl} , R_{Deriv}) were highly correlated with species richness (Figure 4C–D). This initial result concurs with Gould (2000), who showed that variation in NDVI, similar to a derivative because it normalizes for brightness effects in the visible and near IR bands, is significantly

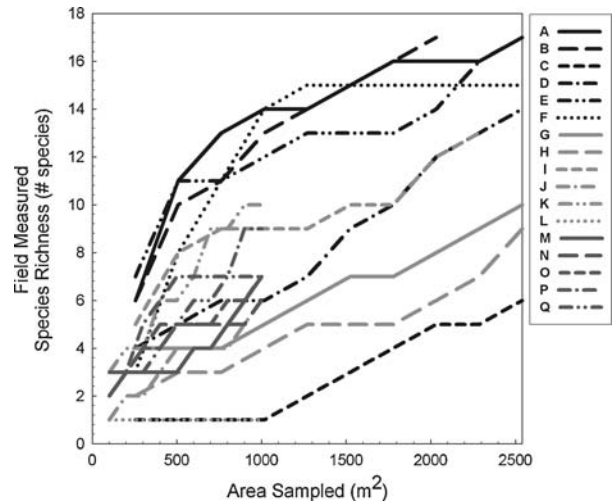


Figure 2. Species-area curves for each field site A–Q described in Table 1.

correlated with vascular species richness in the Arctic tundra. For R_{Refl} , a metric of extremes in percent reflectance, wavelengths in the visible and near-IR portions of the spectrum showed the best linear relationships with species richness. For R_{Deriv} , a metric of the most extreme slopes of the reflectance spectra, a wider range of wavelengths were correlated with species richness. These regions include the green edge (500–550 nm) of the visible portion of the spectrum, the red edge (700–800 nm), various water features in the near-IR, and wavelengths throughout a portion of the shortwave-IR region (SWIR; 1,500–1,800 nm). When the same analyses were performed using Shannon diversity H' values in place of species richness, r values for comparisons between diversity and spectral data were consistently lower for all bands and spectral metrics (data not shown). The weaker relationships between H' and spectral variation may be due to the fact that H' gives more weight to rarer species, whereas spectral diversity as measured by range is not weighted.

After determining which R_{Refl} and R_{Deriv} wavelengths were not strongly ($p > 0.01$) correlated with species richness, we eliminated these wavelengths from our analysis. We then examined correlations among remaining R_{Refl} and R_{Deriv} wavelengths. Pearson’s correlation analysis demonstrated that all remaining wavelengths were highly correlated in reflectance space, but not highly correlated once we converted the spectra to derivatives. That is, Pearson’s correlation coefficients (r) ranged from 0.63 to 0.99 (mean = 0.93) for all comparisons between R_{Refl} wavelengths, but were much lower ($r = 0.10–0.98$, mean 0.70) for

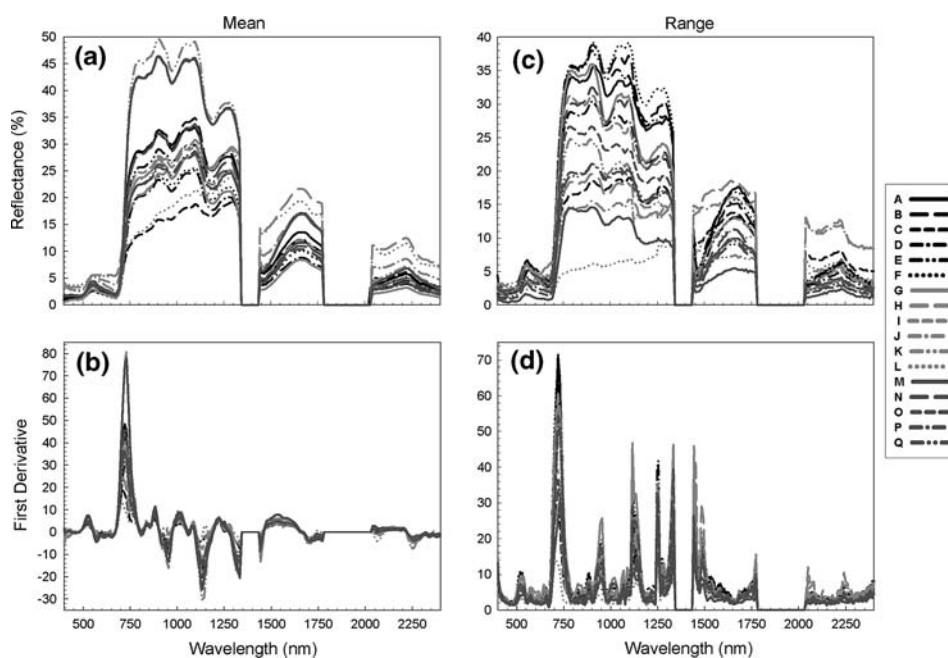


Figure 3. (a–b) Mean reflectance and derivative-reflectance spectrum of each study site; (C–D) Range of reflectance and derivative-reflectance spectrum of each study site.

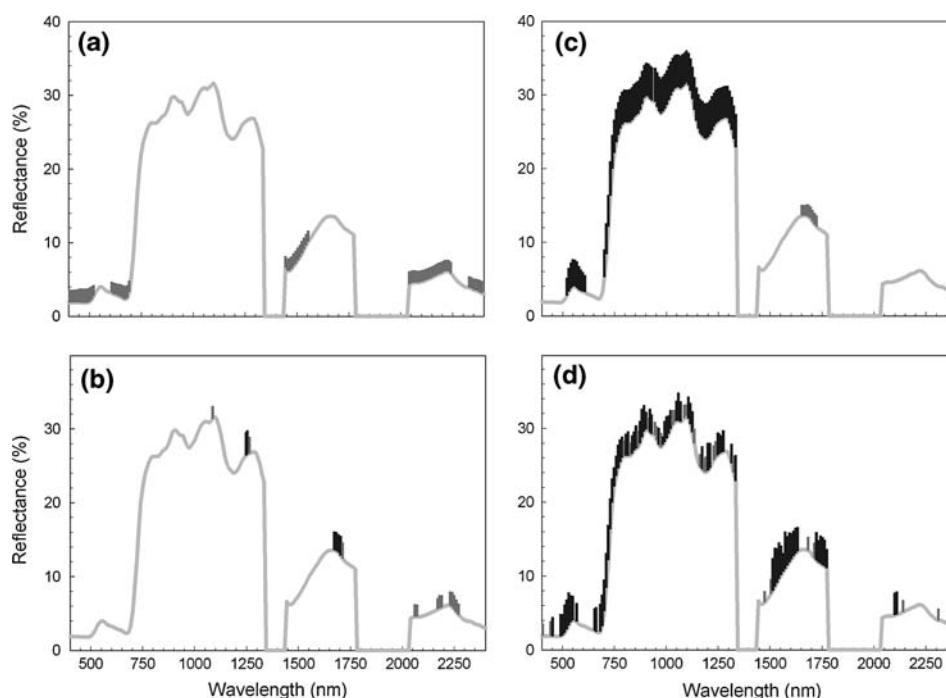


Figure 4. Pearson correlation coefficients between field-based woody species richness and AVIRIS spectral band for **A** mean reflectance, **B** derivative reflectance, **C** reflectance range, and **D** derivative reflectance range. Significance of these relationships varies across the spectrum; *black marks* indicate $p < 0.01$, *grey marks* indicate $0.01 \leq p < 0.05$, and no mark indicates $0.05 \leq p$. The *height of the mark* indicates the magnitude of the Pearson correlation value (r), with taller marks having higher values. The spectrum over which these coefficients are graphed is a mean spectrum derived from all plot areas in this study.

comparisons between R_{Deriv} wavelengths. We therefore concluded that the range of the spectral derivative provided more information than the range of spectral reflectance values.

Leaf Biochemical Variation

If leaf biochemical variation within species exceeds the variation observed among species, then

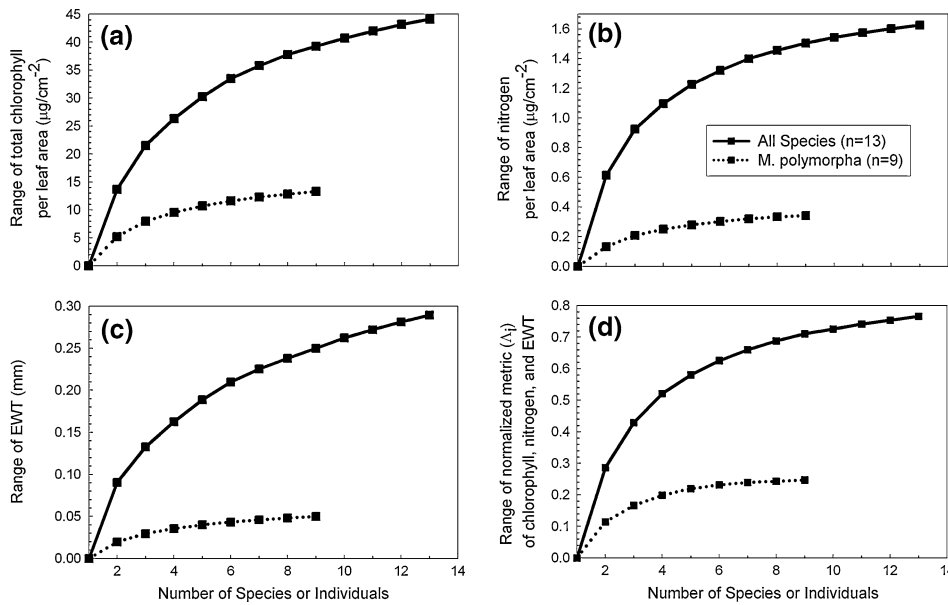


Figure 5. Change in the value range of **A** total chlorophyll, **B** nitrogen, and **C** equivalent water thickness (EWT) in leaves of all species sampled (*solid line*) and *Metrosideros polymorpha* (*dotted line*) across study sites. Panel **(D)** shows the increase in the range of a leaf biochemical metric that combines water, chlorophyll and nitrogen measurements (equation 1 in main text).

variation in AVIRIS spectra within a site is probably not directly related to species richness. In this case, variations in AVIRIS spectral signatures within a site are probably due to leaf biochemical and canopy structural variation among only a few dominant species. On the other hand, if inter-species variation in leaf biochemical properties far exceeds that of within-species variation, and if this occurs at all levels of species richness ($n = 2, 3, \dots, 17$), then it is likely that AVIRIS is measuring species richness by way of the leaf chemical determinations.

Results from the Monte-Carlo analysis, which repeatedly calculated the range of the leaf properties as each new species is randomly added to a community, indicated a non-linear increase in biochemical variation with increasing species richness (solid lines Figure 5). A similar analysis, but using multiple samples from a single species (*M. polymorpha*) taken across 9 of the 17 sites, showed that the range of leaf biochemical values increases much more slowly for a single species than for a mix of different species (dotted lines Figure 5). In other words, inter-specific variation far exceeded intra-specific variation of a single species across sites. The selection model used in this calculation did not consider the fact that species assemblages and biochemical properties in nature are not usually random (for example Ollinger and Smith 2005), but the random addition of species actually makes the test more stringent because it does not take into account the spatial autocorrelation that often simplifies remote sensing analyses. We also note that the range of leaf properties in *M. polymorpha* more clearly reached an asymptote when accumulated

from different field sites, particularly for leaf EWT and N, whereas the range continued to grow as different species were pooled together (the solid lines in Figure 5 never reach an asymptote).

These results provide a good indication that, as biochemical variation (range) increases, so does spectral variation in the particular wavelength regions highlighted in Figure 4. This is only a general attempt to link leaf biochemistry to spectral variation and species richness; we intend to further test these inter-relationships in the field by adding leaf measurements from additional species as well as canopy structural data including leaf area index. However, we found that it is exceedingly difficult to assign specific leaf/canopy properties to specific AVIRIS spectra within a site due to the high spatial heterogeneity of the forest stands and the inaccuracies of co-locating ground and remote sensing data sets (even given the high precision D-GPS and airborne inertial navigation data used in this study). The statistically-based approach presented here at least provided an indication that increasing spectral diversity is linked to increasing species richness by way of increasing biochemical diversity.

Diversity Prediction Algorithm

Based on observations that the shape of the spectrum (R_{Deriv}) and its range are well correlated with species richness, and an understanding of how variation in multiple leaf-level properties increases with species richness, we developed a biodiversity prediction equation for lowland tropical forests in the Puna region. The range of derivative reflectance

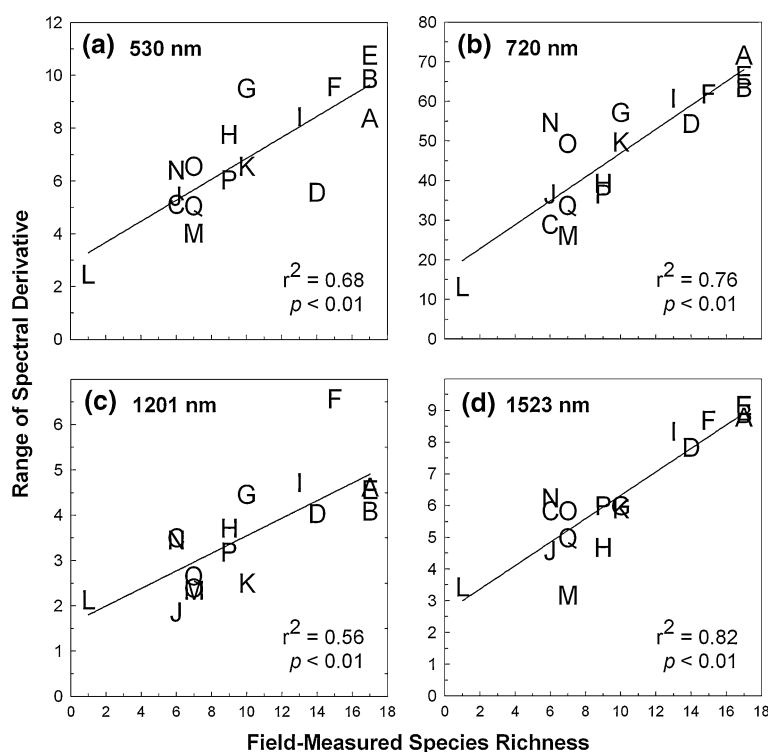


Figure 6. Linear regressions between field-measured woody species richness across all study sites and the derivative-reflectance range at **A** 530, **B** 720, **C** 1,201, and **D** 1,523 nm.

within field sites, and not the range of reflectance, was used because wavelengths significantly correlated with species richness were less intercorrelated using the R_{Deriv} than the R_{Ref} metric (from Figure 4). Lower intercorrelation implies that derivatives provided a greater number of independent variables than did the reflectance measurements. Ideally, each derivative feature that is significantly related to species richness represents some biophysical vegetation feature. Therefore, a greater number of independent variables suggest that more biophysical features were represented by the range of the derivative spectra. Furthermore, a diversity prediction algorithm sensitive to differences in many biophysical properties would be more sensitive to variation in species richness than an algorithm based on only one or two biophysical properties.

Using the linear regression, we examined how variation at a key set of wavelengths was correlated with species richness (Figure 6). We chose wavelengths from portions of the spectrum influenced by three leaf biochemical properties: total chlorophyll, water, and N. These leaf characteristics were associated with species richness as demonstrated by the Monte-Carlo analysis. Variations in these three leaf properties affect the shape of the reflectance spectra as follows: chlorophyll, an upper-canopy leaf pigment, influences the shape of the visible spectrum from 500–550 and 700–800 nm; leaf water, a component of canopy water content,

influences the shape of the water feature from 1,140–1,250 nm, and both leaf water and nitrogen influence the shape of the spectrum in a portion of the SWIR region from 1,500 to 1,700 nm (Curran 1989; Jacquemoud and others 1996; Asner and Vitousek 2005; Ustin and others 2004). Within these four regions, we selected the wavelength with the highest r value for Pearson's correlation analysis between species richness and R_{deriv} : 530, 720, 1,201, and 1,523 nm.

Whereas the reflectance at these wavelengths responds to different biochemical properties, each were correlated with species richness, albeit in different ways. At 530 nm (Figure 6A), the slope of the spectrum is dominated by the chlorophyll absorption feature in upper canopy leaves. Field site D, dominated by the Australian nitrogen-fixing tree *C. equisetifolia*, was the most significant outlier when using the 530 nm spectral slope alone, yielding a narrower range of spectral values than measured species richness. At 720 nm (Figure 6B), the shape of the red edge is dominated by a second chlorophyll absorption, as well as by canopy structure and fluorescence. Field site N, a near-monotypic stand of non-native *P. cattleianum*, is an outlier here; relative spectral variation at this site was greater than measured species richness. The reflectance derivative near 1,201 nm is most sensitive to total canopy water content (Roberts and others 2004). In this regression (Figure 6C),

relative spectral shape variation at field site F, a diverse *M. polymorpha*-dominated stand ($H' = 2.0$), was greater than field-based species richness measurements. At 1,523 nm (Figure 6D), the region where the range of derivative reflectance was most highly correlated with species richness ($r^2 = 0.82$, $p < 0.01$), field site M was the significant outlier. This site, which has relatively lower spectral variation than measured species richness, is dominated by the non-native nitrogen-fixing tree *F. moluccana*, as well as other non-native species.

Although these simple approaches predicted richness relatively well in our particular data set, application of these single-wavelength metrics to other forest stands may be limited because the shape of the curve at any one wavelength (for example 1,523 nm) gives information about only a small number of leaf or canopy properties (Curran 1989; Jacquemoud and others 1996). Single-wavelength observations do not provide a measurement of multiple biochemical (for example pigments) or structural (for example LAI, canopy water content) properties that might, in combination, best indicate variation in species richness by the ensemble of leaf and canopy parameters expressed in a hyperspectral signature.

To broaden the applicability of the AVIRIS observations for biodiversity monitoring, we used a regression model to predict diversity using R_{Deriv} values from four distinct wavelength regions across the spectrum (equation 2):

$$\text{Richness} = 0.44R_{d530} + 0.032R_{d720} + 0.25R_{d1,201} + 1.4R_{d1,523} - 4.2 \quad (2)$$

The spatial variation (range) of the reflectance-derivative spectra at 530, 720, 1,201, and 1,523 nm linearly predicted woody species richness with surprisingly high precision ($r^2 = 0.85$; $p < 0.01$) and accuracy (slope = 0.83, y -intercept = 1.6) (Figure 7). Although R_{Deriv} at 1,523 nm carried the most weight in the regression (equation 2), and variations in the reflectance derivative spectrum at each of these wavelengths were inter-correlated at r^2 values of approximately 0.3–0.8 (Table 2), each wavelength added additional information that made the diversity prediction slightly more robust overall and potentially more widely applicable to new environments.

Diversity Mapping

Our calculated species richness map, covering five forest reserve areas in the Puna region, is shown in Figure 8. Within protected forest reserves, diversity

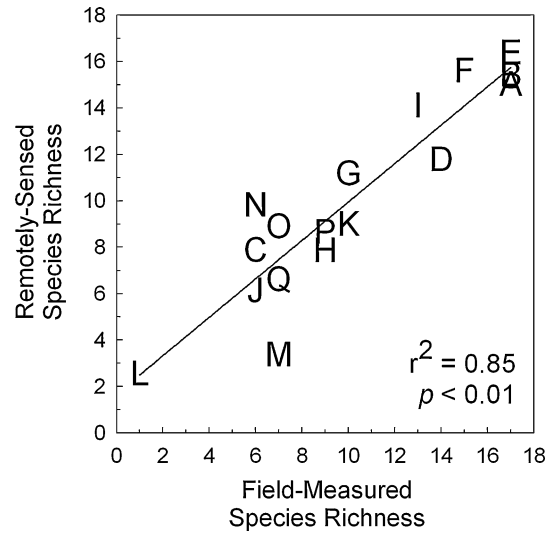


Figure 7. Field-measured richness of woody species in comparison to AVIRIS-predicted richness using multiple linear regression analysis (equation 2, main text) on a per-site basis.

Table 2. Pearson Correlation Coefficients (r) between Woody Species Richness (RICH) and the AVIRIS Reflectance-derivatives at 530 nm and 720 nm (pigments), 1,201 nm (canopy water), and 1,523 nm (leaf water/nitrogen)

Variable	RICH	R_{d530}	R_{d720}	$R_{d1,201}$	$R_{d1,523}$
RICH	–				
R_{d530}	0.84	–			
R_{d720}	0.87	0.87	–		
$R_{d1,201}$	0.77	0.74	0.70	–	
$R_{d1,523}$	0.91	0.81	0.90	0.79	–

Relationships are significant at the $p < 0.01$ level.

tended to scale with substrate age. Young lava flows were distinct because of their low species richness, whereas older forested areas had higher species richness. Averaging over each reserve, we found that richness ranged from 8.6 to 13.2 woody canopy species per 0.1 ha (Table 3). The lowest richness (8.6 ± 3.8 per 0.1 ha) was observed in Keauohana Forest Reserve on young basalt substrates, whereas the highest richness (13.2 ± 2.3 per 0.1 ha) was mapped across the Keaukaha Military Reservation (KMR) on the oldest soils (Table 1). Here, we present a species richness mapping method in reserves as proof-of-concept, and will consider non-reserve areas with potentially high conservation value in upcoming studies.

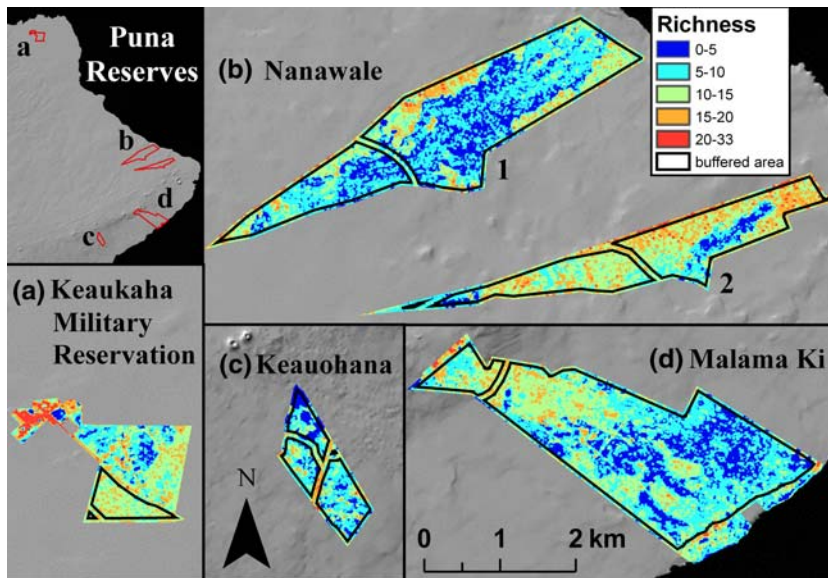


Figure 8. Predicted species richness per 0.1 ha across five forested reserve areas in lowland tropical forests in Hawaii. *Black outlines* denote areas inside which average species richness values were calculated. Areas outside of black lines were excluded due to edge effects.

Table 3. Predicted Species Richness per 0.1 ha (means \bar{X} and standard deviations *sd*) and Area Sampled, across Five Reserve Areas in the Puna Region

Reserve	\bar{X}	Sd	Area Sampled (km ²)
Keaukaha Military Reservation	13.18	2.28	0.30
Keauohana	8.64	3.78	0.77
Malama Ki	9.00	3.73	5.12
Nanawale 1	8.66	4.02	4.25
Nanawale 2	12.78	4.16	2.17

CONCLUSIONS

Biological diversity is a central determinant of ecosystem function and a key contributor to the portfolio of services provided by ecosystems to humans. Rapid changes in biodiversity are taking place around the world, due in large part to land-use change, climate change, and introduced species, among other factors (Sala and others 2000). Methods are needed to map and monitor aspects of biodiversity, but remote sensing approaches thus far usually focus on basic delineation of land-cover types without directly resolving the biochemical or structural properties of the vegetation most closely linked to taxonomic diversity. Moreover, there is a need for high-resolution biodiversity mapping and monitoring in support of ecosystem service assessments in the conservation, management and policy development arenas. Very few, if any, operational

methods have been developed for quantifying biodiversity at high spatial resolution at regional scales.

We sought to advance the use of airborne imaging spectroscopy for mapping biodiversity in lowland tropical forests on the island of Hawai'i. The biodiversity map developed here defines only woody vascular plant species richness. However, past research has shown that other types of diversity (for example arthropod), as well as ecosystem processes such as plant productivity, may be associated with plant diversity (Siemann and others 1998; Schlapfer and Schmid 1999). Because of the high spatial resolution of the airborne imagery (~3.6 m), land managers can use image results such as ours to track changes in diversity over time and potentially identify diversity hotspots of particular conservation interest.

In Hawaii, species mapping is especially important because invasion by exotic organisms is currently one of the greatest threats to maintenance of native diversity throughout the archipelago (Smith 1985; Vitousek 1990). Our diversity maps do not explicitly consider the distribution of non-native species across the landscape. Additional mapping techniques, such as image classification using unique spectral and biochemical signatures, are more appropriate to map individual species (Asner and Vitousek 2005; Clark and others 2005).

The overall diversity mapping approach developed here may be appropriate for other forests for which hyperspectral imagery is available, and where the spatial resolution of the imagery is appropriate to the scale of diversity being mapped. However, the species richness prediction algorithm developed in this study may not be applied directly

to other areas or different vegetation regimes; the Puna region is relatively unique because of its very young substrates and moderate species richness, and this algorithm may depend on these distinctive regional attributes to calculate diversity. In a different forest type, different spectral regions or wavelengths may be better correlated with species richness. Hyperspectral data are therefore a key component to this type of diversity mapping, because fine spectral resolution allows great flexibility in wavelength choice not available from multispectral data.

It is also important to note that the reflectance-derivative range method relies on the use of high-fidelity hyperspectral data. More noisy data, such as those generated by other hyperspectral sensors (for example EO-1 Hyperion), will probably provide ambiguous results in comparison to the very high-fidelity AVIRIS spectra (Townsend and Foster 2002). Furthermore, biodiversity assessment based on range is sensitive to outliers due to atmospheric contamination and artifacts such as high frequency noise along the edges of water bands, factors which may result in increased reflectance and derivative-reflectance ranges. Additional research is required to test our approach in other ecosystems and with other hyperspectral sensors. Nevertheless, biodiversity predictions based on ranges of reflectance derivative values in wavelength regions of the spectrum associated with an ensemble of canopy biochemical and structural properties, and constrained by a small set of ground surveys, is a robust method of estimating species richness across a range of ecological communities in Hawai'i and elsewhere.

One of the most important results of this study, that leaf-level variation in pigment concentrations, N, and water concentration scales with the number of species analyzed, forms an important connection between the hyperspectral reflectance-derivative signatures and the species richness data. The relationship suggests that the spectral variation measured by AVIRIS is largely caused by inter-specific variation in leaf biochemical properties. The next step in the effort to connect ground data to remotely sensed data via leaf properties such as pigment, nitrogen and water content, is to collect these data from more species and to scale the biochemical data upward based on the actual canopy (crown) areas. This is a daunting task in tropical forest environments, but with leaf chemistry and structure information scaled to canopy area, we could more closely examine how leaf-level variation interacts with species richness and remotely sensed spectral variation. Future remote sensing studies of biodiversity will benefit from explicitly

connecting chemical and physical properties of the organisms in question with remote sensing data. These efforts will require the appropriate remote sensing data, such as from high performance hyperspectral sensors, collected at spatial resolutions commensurate with land management and conservation goals. Such analyses will also allow us to better understand why and how diversity at multiple scales, from intra-specific genetic diversity to regional beta diversity, can be effectively mapped by both airborne and spaceborne sensors.

ACKNOWLEDGMENTS

We thank R. Mudd, C. Perry, and G. Sanchez for assistance in the field, and N. Zimmerman for providing previously unpublished data. Special thanks to M. Eastwood, R. Green, and the AVIRIS team. Access to field sites was provided by State of Hawaii Division of Forestry and Wildlife, Hawaii Army National Guard, and Kamehameha Schools. This study was undertaken as part of the joint Carnegie-IPIF Hawaiian Ecosystem Dynamics and Invasive Species program, and was supported by NASA Terrestrial Ecology and Biodiversity Program grant NNG-06-GI-87G, The Carnegie Institution, and the U.S. Forest Service. This material is based upon work supported in part by the National Science Foundation under Grant No. 0237065. Any opinions, findings, and conclusions or recommendations expressed in this material are those of the authors and do not necessarily reflect the views of the National Science Foundation.

REFERENCES

- Asner GP, Elmore AJ, Hughes RF, Warner AS, Vitousek PM. 2005. Ecosystem structure along bioclimatic gradients in Hawaii from imaging spectroscopy. *Remote Sens Environ* 96:497–508.
- Asner GP, Vitousek PM. 2005. Remote analysis of biological invasion and biogeochemical change. *Proc Natl Acad Sci USA* 102:4383–6.
- Clark M, Roberts DA, Clark DB. 2005. Hyperspectral discrimination of tropical rain forest tree species at leaf to crown scales. *Remote Sens Environ* 96:375–98.
- Cochrane MA. 2000. Using vegetation reflectance variability for species level classification of hyperspectral data. *Int J Remote Sens* 21:2075–87.
- Cohen WB, Spies T. 1990. Semivariograms of digital imagery for analysis of conifer canopy structure. *Remote Sens Environ* 34:167–178.
- Curran PJ. 1989. Remote sensing of foliar chemistry. *Remote Sens Environ* 30:271–8.
- Gaston KJ. 2000. Global patterns in biodiversity. *Nature* 405:220–227.
- Giambelluca TW, Nullet MA, Schroeder TA. 1986. Rainfall atlas of Hawaii. Honolulu (HI). State of Hawaii: Department of Land and Natural Resources, p 267.

- Givnish TJ. 1999. On the causes of gradients in tropical tree diversity. *J Ecol* 87:193–210.
- Gotelli NJ, Colwell RK. 2001. Quantifying biodiversity: procedures and pitfalls in the measurement and comparison of species richness. *Ecol Lett* 4:379–391.
- Gould W. 2000. Remote sensing of vegetation, plant species richness, and regional biodiversity hotspots. *Ecol Appl* 10:1861–70.
- Green RO, Eastwood ML, Sarture CM, Chrien TG, Aronsson M, Chippendale BJ, Faust JA, Pavri BE, Chovit CJ, Solis M, Olah MR, Williams O. 1998. Imaging spectroscopy and the airborne visible/infrared imaging spectrometer (AVIRIS). *Remote Sens Environ* 65:227–248.
- Heywood VH, Watson RT, Eds. 1995. *Global biodiversity assessment*. Cambridge: Cambridge University Press, p 1140.
- Hughes RF, Denslow JS. 2005. Invasion by a N₂-fixing tree alters function and structure in wet lowland forests of Hawaii. *Ecol Appl* 15:1615–28.
- Innes JL, Koch B. 1998. Forest biodiversity and its assessment by remote sensing. *Glob Ecol Biogeogr Lett* 7:397–419.
- Jacquemoud S, Ustin SL, Verdebout J, Schmuck G, Andreoli G, Hosgood B. 1996. Estimating leaf biochemistry using the PROSPECT leaf optical properties model. *Remote Sens Environ* 56:194–202.
- Johnson DDP, Hay SI, Rogers DJ. 1998. Contemporary environmental correlates of endemic bird areas derived from meteorological satellite sensors. *Proc R Soc B: Biol Sci* 265:951–59.
- Lichtenthaler HK. 1987. Chlorophyll and carotenoids: pigments of photosynthetic membranes. *Meth Enzymol* 148:350–87.
- Lichtenthaler HK, Buschmann C. 2001. Chlorophylls and carotenoids: measurement and characterization by UV-VIS spectroscopy. In: Wrolstad RE, Ed. *Current protocols in food analytical chemistry*. New York: Wiley. pp F4.3.1–F4.3.8.
- Martin ME, Aber JD. 1997. High spectral resolution remote sensing of forest canopy lignin, nitrogen, and ecosystem processes. *Ecol Appl* 7:431–43.
- McGrew JC, Monroe CB. 2000. *An introduction to statistical problem solving in geography*. Dubuque (IA): McGraw-Hill, p 264.
- Moore RB, Trusdell FA. 1991. Geologic map of the lower east rift zone of Kilauea Volcano, Hawaii. U.S. Geologic Quadrangle Map GQ-667, scale 1:24,000.
- Mueller-Dombois D, Fosberg FR. 1998. *Vegetation of the tropical Pacific Islands*. New York: Springer, p 733.
- Myers N, Mittermeier RA, Mittermeier CG, da Fonseca DAB, Kent J. 2000. Biodiversity hotspots for conservation priorities. *Nature* 403:853–8.
- Nagendra H. 2001. Using remote sensing to assess biodiversity. *Int J Remote Sens* 22:2377–400.
- Ollinger SV, Smith ML. 2005. Net primary productivity and canopy nitrogen in a temperate forest landscape: an analysis using imaging spectroscopy, modeling, and field data. *Ecosystems* 8:760–78.
- Pielou EC. 1966. The measurement of diversity in different types of biological collections. *J Theor Biol* 13:131–44.
- Rahman AF, Gamon JA, Sims DA, Schmidts M. 2003. Optimum pixel size for hyperspectral studies of ecosystem function in southern California chaparral and grasslands. *Remote Sens Environ* 84:192–207.
- Roberts DA, Ustin SL, Ogunjemiyo S, Greenberg J, Dobrowski SZ, Chen JQ, Hinckley TM. 2004. Spectral and structural measures of northwest forest vegetation at leaf to landscape scales. *Ecosystems* 7:545–62.
- Sala OE, Chapin FS, Armesto JJ, Berlow E, Bloomfield J, Dirzo R, Huber-Sanwald E, Huenneke LF, Jackson RB, Kinzig A, Leemans R, Lodge DM, Mooney HA, Oesterheld M, Poff NL, Sykes MT, Walker BH, Walker M, Wall DH. 2000. Global biodiversity scenarios for the year 2100. *Science* 287:1770–4.
- Schlapfer F, Schmid B. 1999. Ecosystem effects of biodiversity: a classification of hypotheses and exploration of empirical results. *Ecol Appl* 9:893–912.
- Siemann E, Tilman D, Haarstad J, Ritchie M. 1998. Experimental test of the dependence of arthropod diversity on plant diversity. *Am Nat* 152:738–750.
- Smith CW. 1985. Impact of alien plants on Hawaii's native biota. Stone CP, Scott JM, Eds. *Hawaii's terrestrial ecosystems: preservation and management*. Honolulu: Cooperative National Park Resources Study Unit, University of Hawaii. p 180–250.
- Townsend PA, Foster JR. 2002. Comparison of EO-1 Hyperion to AVIRIS for mapping forest composition in the Appalachian Mountains, USA. *Int Geosci Remote Sens Symp* 2:793–5.
- Turner W, Spector S, Gardiner N, Fladeland M, Sterling E, Steininger M. 2003. Remote sensing for biodiversity and conservation. *Trends Ecol Evol* 18:306–314.
- Ustin SL, Roberts DA, Gamon JA, Asner GP, Green RO. 2004. Using imaging spectroscopy to study ecosystem processes and properties. *Biol Sci* 54:523–534.
- Vitousek PM. 1990. Biological invasions and ecosystem processes: towards an integration of population biology and ecosystem studies. *Oikos* 57:7–13.
- Vitousek PM. 2004. *Nutrient cycling and limitation: Hawaii'i as a model system*. Princeton: Princeton University Press, p 232.